

Dynamical aspects of magnetization reversal in the neodymium permanent magnet by a stochastic Landau-Lifshitz-Gilbert simulation at finite temperature: Real-time dynamics and quantitative estimation of coercive force

Masamichi Nishino ^{1,2,*}, Ismail Enes Uysal ², Taichi Hinokihara,^{3,2} and Seiji Miyashita^{3,4,5,2}

¹*Research Center for Advanced Measurement and Characterization, National Institute for Materials Science, 1-2-1 Sengen, Tsukuba, Ibaraki 305-0047, Japan*

²*Elements Strategy Initiative Center for Magnetic Materials, National Institute for Materials Science, 1-2-1 Sengen, Tsukuba, Ibaraki 305-0047, Japan*

³*Department of Physics, Graduate School of Science, The University of Tokyo, 7-3-1 Hongo, Tokyo 113-0033, Japan*

⁴*The Physical Society of Japan, 2-31-22 Yushima, Tokyo 113-0033, Japan*

⁵*Institute for Solid State Physics, The University of Tokyo, 5-1-5 Kashiwanoha, Kashiwa 277-8581, Japan*



(Received 3 June 2020; accepted 17 July 2020; published 30 July 2020)

The Nd magnet, $\text{Nd}_2\text{Fe}_{14}\text{B}$, is an important material because of its high coercivity applied in modern technologies. However, the microscopic mechanism of the coercivity has not been well understood. We study the magnetization reversal of a single grain of the magnet at a finite temperature by a real-time stochastic Landau-Lifshitz-Gilbert simulation of an atomistic model, which enables us to analyze dynamical properties reflecting the atomic-scale magnetic structure. There exist difficulties to estimate long relaxation times of the reversal quantitatively, i.e., the limitation of simulation time and also dependence on the damping factor α . Here we develop a statistical method to estimate precisely long relaxation times in the stochastic region, by which one can identify an initial transient process and a long-time regular relaxation process. The relaxation time is found to largely depend on α especially in the stochastic region. However, it is found that a sharp increase of the relaxation time with lowering an external magnetic field causes a close location of the threshold fields for different values of α . By making use of this fact, we quantitatively estimate the coercive field at which the relaxation time is 1 s.

DOI: [10.1103/PhysRevB.102.020413](https://doi.org/10.1103/PhysRevB.102.020413)

High-performance permanent magnets are indispensable materials in modern technologies. Especially the Nd magnet, $\text{Nd}_2\text{Fe}_{14}\text{B}$ [1–6], is very important because of its high coercive field applied in electric motors, electronic devices, etc. [7]. The coercive field of the Nd magnet is estimated from the viewpoint of the Stoner-Wohlfarth model to be double of the anisotropic constant divided by the saturated magnetization, which is more than 10 T at zero temperature. However, the coercive field at room temperature is less than 3 T. This large reduction of the coercive field pointed out by Kronmüller [8] has been a big topic in the study of permanent magnets. Quantitative estimation of the coercive field theoretically and computationally is a most difficult problem. The mechanism of the coercivity has not been well understood yet [9].

So far, theoretical and computational studies for magnetic properties of permanent magnets have been performed based on models with continuum magnetization, i.e., the micromagnetics, and they have achieved a measure of success in analyses of qualitative aspects of magnetization reversals, estimation of coercive force, etc. [10,11]. However, in such continuum modelings, the microscopic details of crystal structures and magnetic parameters are not introduced, and the thermal fluctuation effect cannot be treated properly. For the understanding of the microscopic mechanisms of coercivity, atomistic modelings at finite temperatures are important.

Recently, an atomistic model for the Nd magnet has been developed to study the finite temperature properties. For the atomistic model, the microscopic parameters are necessary, which were taken either from first-principles calculations [12–23], or from an empirical way [24,25]. Quantitative properties of the magnet mainly focusing on static features have been actively investigated on the temperature dependence of the magnetization [12–15,21], domain wall profiles [13,15,16,21,22], dipolar-interaction effect [14], ferromagnetic resonance [17], inhomogeneity effect [16,18,22–25], free-energy barriers [19], and surface Nd anisotropy effect [20].

In contrast to the static properties, quantitative analyses of the dynamical properties of the magnet by the atomistic model have been scarcely developed. The coercivity is a phenomenon of a magnet, i.e., an ensemble of many magnetic grains. In practice, however, it is not realistic to study by atomistic model approaches. Thus, as a first step to understand this phenomenon, it is important to know how the magnetization of a single grain reverses as a function of an external field. With the use of the Wang-Landau Monte Carlo (MC) sampling method [26], a quantitative estimation of the coercive field of a single grain at a finite temperature has been performed very recently by calculating the free-energy barrier ΔF of an atomistic model [19], with the use of the Arrhenius law for the relaxation time: $\tau = \tau_0 e^{\Delta F}$ under the assumption of $\tau_0 = 10^{-11}$ s [27].

*Corresponding author: nishino.masamichi@nims.go.jp

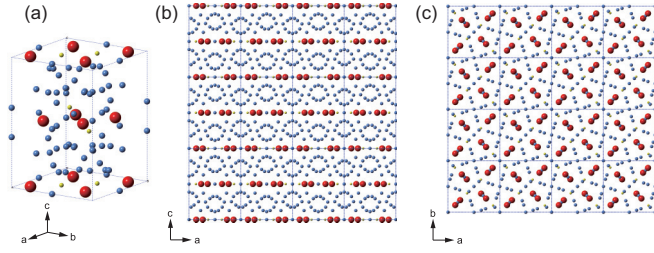


FIG. 1. Unit cell of $\text{Nd}_2\text{Fe}_{14}\text{B}$. Neodymium, iron, and boron atoms are denoted by red, blue, and yellow spheres, respectively. The lattice constants [2] for the a , b , and c axes are $d_a = d_b = 8.80 \text{ \AA}$, and $d_c = 12.19 \text{ \AA}$, respectively. (b) Side view (from the a or b axis). (c) Top view (from the c axis).

However, magnetization reversal is triggered by a nucleation and is accomplished through the growth of domains with reversed magnetization. Thus, real-time dynamics studies are important to catch the mechanism of the coercivity. The stochastic Landau-Lifshitz-Gilbert (SLLG) equation [28,29] can be used for the relaxation dynamics quantitatively thanks to atomistic parameters of the material. By employing this method, we find the nature of domain wall propagation reflecting the microscopic (atomic scale) lattice structure and magnetic parameters. However, practical simulation time is around 1 ns, which is too short to study the coercivity, i.e., a phenomenon of 1 s. The limitation of the simulation time is a common problem for long-time dynamics in real-time simulations with realistic parameters.

Furthermore in the SLLG simulation, the relaxation time depends on the Gilbert damping factor α [29]. Although several attempts to estimate the value of the damping factor have been done [30–39], generally it is difficult to estimate the value of α including temperature and field dependencies both experimentally and theoretically. Indeed, the value of α for the Nd magnet and its temperature and field dependencies are unknown. These difficulties have prevented us from a quantitative estimation of the coercive field even if we use the atomistic parameters.

In the present Rapid Communication, we overcome these difficulties by the following ingenuities. We introduce a statistical method which extends the limitation of the simulation time and makes possible accurate estimation of the relaxation time. Although the relaxation time is found to largely depend on α especially in the stochastic region at low fields, a sharp increase of the relaxation time causes a close location of the threshold fields for different values of α . Making use of this property, we quantitatively estimate the coercive field at which the relaxation time is 1 s by an extrapolation of a fitting function.

The unit cell of the Nd magnet is shown in Fig. 1(a), which consists of Fe, B, and Nd atoms. We use the atomistic Hamiltonian for the Nd magnet [12–14]:

$$\mathcal{H} = - \sum_{i < j} 2J_{ij} \mathbf{s}_i \cdot \mathbf{s}_j - \sum_i^{\text{Fe}} D_i (s_i^z)^2 + \sum_i^{\text{Nd}} \sum_{l,m} \Theta_{l,i} A_{l,i}^m \langle r^l \rangle_i \hat{O}_{l,i}^m - \sum_i H_{\text{ext}} S_i^z. \quad (1)$$

The first term denotes the exchange coupling J_{ij} between the i th and j th sites, the second one is the magnetic anisotropy energy for Fe atoms whose constant is D_i , the third one describes the magnetic anisotropy energy for Nd atoms, and the last term is the Zeeman term. For Fe and B atoms, s_i denotes the magnetic moment at the i th site, while for Nd atoms, it is the moment of the valence ($5d$ and $6s$) electrons. The total moment for Nd atoms at the i th site is $\mathcal{S}_i = s_i + \mathcal{J}_i$, where $\mathcal{J}_i = g_T J_i \mu_B$ with the magnitude of the total angular momentum, $J = 9/2$, and the Landé g factor, $g_T = 8/11$. We define $\mathcal{S}_i = s_i$ for Fe and B atoms. The details of the model are given in our previous papers [12–14].

To study magnetization reversal dynamics, we apply the SLLG equation [17,28,29]:

$$\frac{d}{dt} \mathbf{S}_i = - \frac{\gamma}{1 + \alpha_i^2} \mathbf{S}_i \times (\mathbf{H}_i^{\text{eff}} + \boldsymbol{\xi}_i) - \frac{\alpha_i \gamma}{(1 + \alpha_i^2) S_i} \mathbf{S}_i \times [\mathbf{S}_i \times (\mathbf{H}_i^{\text{eff}} + \boldsymbol{\xi}_i)]. \quad (2)$$

Here α_i is the Gilbert damping factor at the i th site, γ is the gyromagnetic constant, $\mathbf{H}_i^{\text{eff}} = - \frac{\partial \mathcal{H}}{\partial \mathbf{S}_i}$ is the effective field applied at the i th site from the exchange interactions and the anisotropy terms, and $\boldsymbol{\xi}_i$ is a white-Gaussian noise. The temperature of the system is a function of the strength of the random noise field \tilde{D}_i :

$$\tilde{D}_i = \frac{\alpha_i k_B T}{S_i \gamma}. \quad (3)$$

We assume that the damping factor does not depend on site, i.e., $\alpha_i = \alpha$. We apply a kind of middle-point method [29] equivalent to the Heun method [28] for the numerical integration in Stratonovich interpretation. For the time step of this equation, $\Delta t = 0.1 \text{ fs}$ is used.

Throughout this Rapid Communication we study a system of $12 \times 12 \times 9$ unit cells along the a , b , and c axes, respectively, which has an approximately cubic shape ($10.56 \text{ nm} \times 10.56 \text{ nm} \times 10.971 \text{ nm}$), with open boundary conditions. The side view from the a or b axis and the top view of $4 \times 4 \times 3$ unit cells are given in Figs. 1(b) and 1(c), respectively.

In our atomistic model, the magnetic transition (Curie) temperature was estimated to be around $T_C = 870 \text{ K}$, which is a little overestimated from the experimental values ($\sim 600 \text{ K}$) due to an overestimation of the exchange interactions [12,13]. We are interested in room temperature properties and set $T = 400 \text{ K} \simeq 0.46 T_C$, which is close to room temperature practically.

In Fig. 2 we show snapshots of the magnetization reversal from the down-spin state for $\alpha = 0.1$ under a reversed field, $h = 4.0 \text{ T}$, which is in the stochastic region. The system is relaxed from the down-spin state (the first panel of Fig. 2).

There, we find that the nucleation occurs from a corner, and a magnetic domain with reversed magnetization grows parallel to the ab plane (see also Fig. 1) and then grows in the direction of the c axis. This is because the effective exchange interactions along the a or b axis are stronger than those along the c axis [13,16]. The nucleus earns an energy gain, i.e., lower energy by expanding parallel to the ab plane. Thus, first the domain wall (this is a Bloch wall) of the corner domain moves parallel to the ab plane, and then the domain wall (this

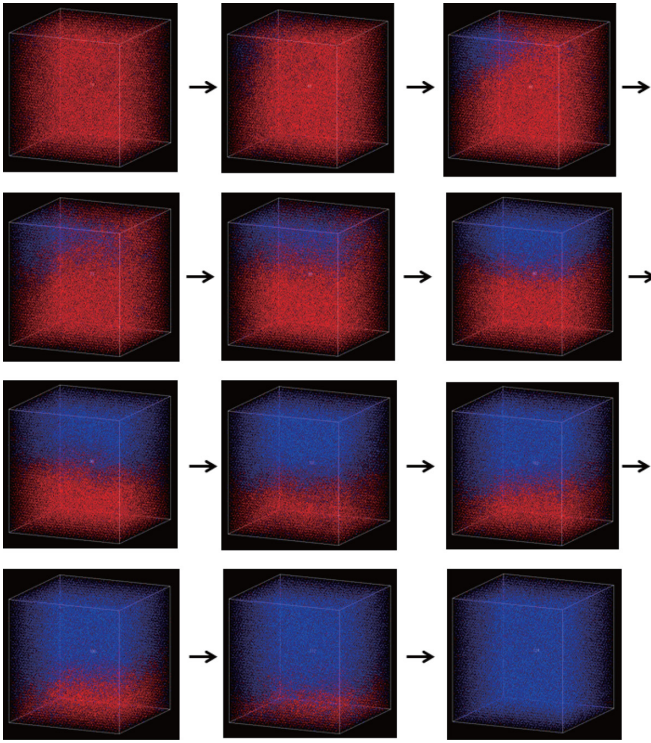


FIG. 2. Snapshots of the magnetization reversal from the all-down spin state under a reversed field ($h = 4.0$ T). Red and blue parts denote down-spin and up-spin states, respectively.

is a Néel wall) moves in the direction of the c axis. We observe that this tendency is independent of the value of α .

Under a reversed field, the magnetization relaxation is observed. We measure the time dependence of the per-site magnetization,

$$m_z = \frac{1}{N_{\text{site}}} \sum_{i=1}^{N_{\text{site}}} S_i^z, \quad (4)$$

where N_{site} is the number of the atoms in the system.

In magnetization reversal there are two typical types of relaxation, i.e., the deterministic one for large fields, which is characterized by the multinucleation Avrami process, and the stochastic one for small fields, which is characterized by a single nucleation, and the border between them is called the dynamical spinodal point [40].

In Fig. 3, we depict the time dependence of the magnetization in samples of the relaxation process for $\alpha = 0.1$ at (a) $h = 8$ T and (b) $h = 4.1$ T. At $h = 8$ T the samples show short relaxation times, and they are the deterministic type, while at $h = 4.1$ T the samples give large relaxation times, and they are the stochastic type. In Fig. 3(b), a few samples do not relax, and thus it is impossible to estimate the average relaxation time until they relax. A large distribution of the relaxation time prevents us from a practical estimation of the average relaxation time. To overcome this difficulty, we introduce a statistical method to evaluate the relaxation time.

We derive the statistical relation between the reversal probability and the relaxation time. If an event (relaxation) occurs with a probability p in a unit time, the probability to

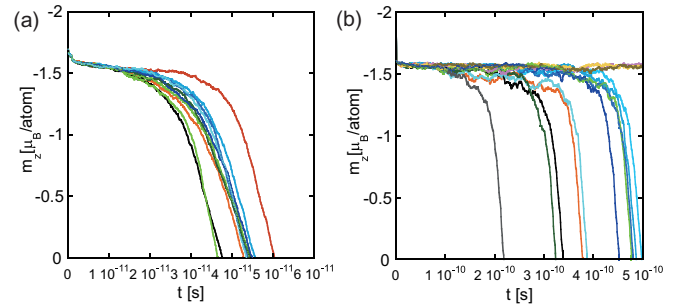


FIG. 3. Examples of magnetization relaxation curves with time dependence at (a) $h = 8$ T and (b) $h = 4.1$ T. $\alpha = 0.1$.

have the event for the first time in the period $[t, t + \Delta t]$ is $(1 - p\Delta t)^{t/\Delta t} p\Delta t = pe^{-pt} \Delta t$. The mean relaxation time $\langle \tau \rangle$ is given by

$$\langle \tau \rangle = p \int_0^\infty t e^{-pt} dt = \frac{1}{p}. \quad (5)$$

The probability $P(t)$ to have the event in the period $[0, t]$ is $P(t) = 1 - e^{-pt}$. If we perform N times simulations, the number of the survival (unchanged) samples is $N_{\text{sv}}(t) = N - N_{\text{done}}(t) = Ne^{-pt}$. Then, p (and τ) can be estimated from the slope of $\ln[N_{\text{sv}}(t)/N]$ versus $-pt$.

We carry out simulations of $N = 864-2592$ samples. In Fig. 4 we show the time dependence of $\ln(N_{\text{sv}}/N)$ for $\alpha = 0.1$ at (a) $h = 8$ T and (b) $h = 4.1$ T. We find that the function $\ln(N_{\text{sv}}/N)$ shows an upward-convex curve in an early period and after this period it exhibits a straight line. This suggests that, in both cases, in the early stage of the relaxation process from the all-down state, some additional time is needed. For longer time, the process is governed by a nucleation rate. Thus, the present method has a merit to identify the initial transient process which causes a bias in the simple average of the relaxation time.

We perform a linear least-square fitting (red lines in Fig. 4) to the straight part to estimate the slope for Figs. 4(a) and 4(b) and obtain $p = 2.697 \times 10^{11}$ [1/s] and $p = 1.491 \times 10^9$ [1/s], respectively. Using the relation (5), the relaxation time is obtained as $\tau = 3.71 \times 10^{-12}$ s and $\tau = 6.71 \times 10^{-10}$ s for Figs. 4(a) and 4(b), respectively. In the same way, we estimate

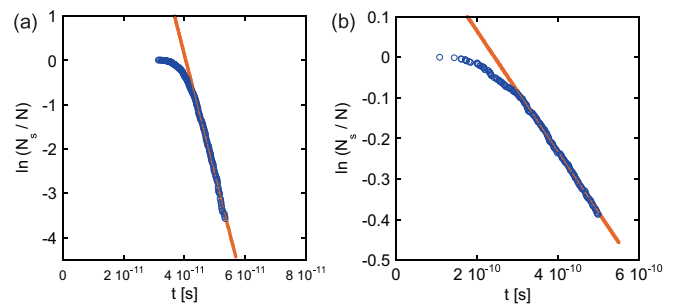


FIG. 4. Time dependence of $\ln(N_{\text{sv}}/N)$. Blue circles denote time dependence of $\ln(N_{\text{sv}}/N)$ at (a) $h = 8$ T and (b) $h = 4.1$ T. $\alpha = 0.1$. For (a) and (b), the slopes $p = 2.697 \times 10^{11}$ 1/s and $p = 1.491 \times 10^9$ 1/s are estimated, respectively, by linear fitting (red lines). Details are given in the text.

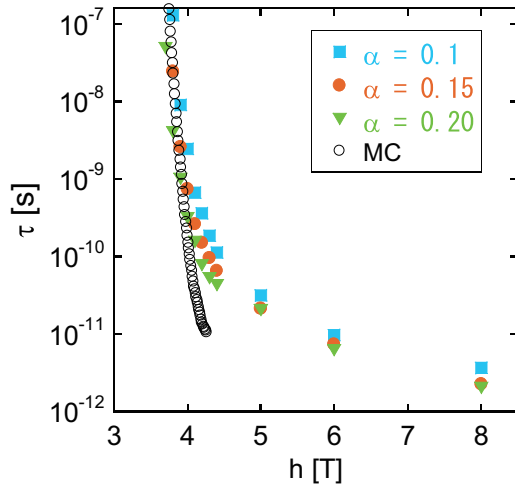


FIG. 5. Magnetic field dependence of the relaxation time (magnetization reversal time) with the damping factor α dependence. The open circles denote the relaxation time of the Arrhenius law ($\tau = \tau_0 e^{\Delta F}$), in which ΔF is the data of Fig. 1(b) in a Monte Carlo study [19]. Details are given in the text.

τ for different values of the external field and damping factor, which are depicted in Fig. 5.

The relaxation time increases steeply below around 4.2 T. However, the relaxation time depends on the value of damping factor α , and we find that the dependence in the stochastic region (low fields) is larger than that in the deterministic region (high fields). Due to this significant dependence of the relaxation time on α , it is difficult to estimate quantitatively the relaxation time without information of the value of α . However, because of the sharp increase of the relaxation times in the stochastic region, the threshold fields for all values of the damping factor are located in a narrow region of the field for a given relaxation time, which allows us to estimate the typical value of the threshold field quantitatively.

To examine this feature, we plot the field dependence of the relaxation time for each value of α with a double exponential fitting, i.e., the Arrhenius law with a correction term:

$$\tau(h) = Ae^{-ah} + Be^{-bh} = Ae^{-ah}(1 + Ce^{-dh}), \quad (6)$$

where $C = B/A$ and $d = b - a$. Concretely, we determine the parameters A, a, C, d by minimizing the cost function:

$$\chi_2 = \sum_k \frac{1}{\sigma_k^2} \{ \log_{10}[\tau(h_k)] - \log_{10}[Ae^{-ah_k}(1 + Ce^{-dh_k})] \}^2, \quad (7)$$

where $\tau(h_k)$ is the values obtained by the simulation for a given value of the field h_k .

Here we take the smallest four values of h_k ($k = 1-4$) at which τ is large. We adopt $\sigma_k = 1$ for simplicity. For large values of $\tau(h_k)$, σ_k should be small, but we confirmed that this dependence on the estimation is small. In Fig. 6, the fitted curves of Eq. (6) are plotted for different values of α . The intersection of each line with $\tau = 1$ s gives the expected coercive field. The estimated values of the coercive field for $\alpha = 0.1, 0.15,$ and 0.2 are $h_c \simeq 3.2, 3.0,$ and 3.0 , respectively, and we find that the coercive field is around 3 T, $h_c \simeq 3$ T. This value is close to $h_c \simeq 3.3$ T, estimated from $\tau = 10^{-11} e^{\Delta F}$

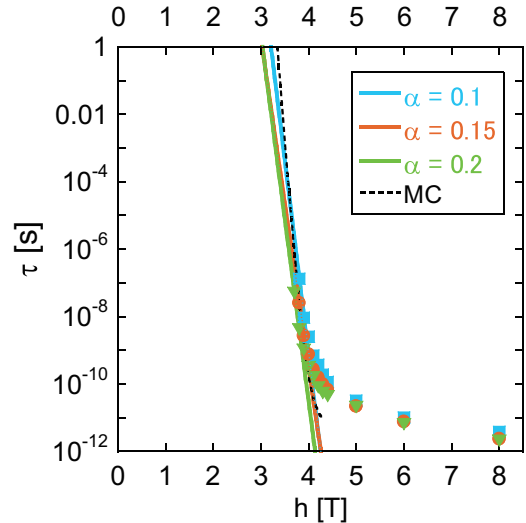


FIG. 6. Extrapolation of the relaxation time for different values of the damping factor for the estimation of the coercive field. The dashed line denotes the relaxation time of the Arrhenius law ($\tau = \tau_0 e^{\Delta F}$), in which ΔF is the data of Fig. 1(b) in a Monte Carlo study [19].

with the free-energy barrier by the MC method [19] (dashed line in Fig. 6). We find that, although the simulation time of the dynamical equation is limited and much shorter than 1 s, the extrapolation of the relaxation time using a fitting function as $\tau(h)$ is available for the estimation of the coercive force.

In summary, in the real-time simulation we found a characteristic nucleation dynamics of the Nd magnet, i.e., a corner nucleation and a magnetic domain growth which reflects the orientation dependence of the exchange interactions [13,16]. This is independent of the values of the damping factor (α). We introduced a useful method to estimate the average relaxation time by evaluating the average reversal probability from many samples, which relieved the difficulty of the estimation due to the wide distribution of the relaxation time. This method overcomes the limitation of the simulation time and also matches well parallel computing. Furthermore, this has another advantage for getting rid of an early period affected by the initial state, and it enables us to identify the regular relaxation region for the accurate estimation of the average relaxation time. We found that the relaxation time largely depends on the value of α in the stochastic region. However, because of the rapid increase of the relaxation time in the stochastic region, the threshold fields for different values of α for a long relaxation time are located in a small range. This fact allows us to estimate the coercive force quantitatively, even if the value of α is unknown. In this method there is no need to introduce the attempt time τ_0 used in the Arrhenius formula.

In the present study we did not take into account the effect of the dipolar interaction, which does not affect the magnetization reversal practically at 10 nm scale. In a larger system (many grains) this effect becomes important, but such a long-range interaction is difficult to study, which is left for a challenging problem in the future.

This Rapid Communication presented a method to estimate the coercive force quantitatively with a realistic atomistic

model at a finite temperature by direct real-time simulation, which will advance studies on the mechanism of the coercivity.

The authors would like to thank Dr. Hirosawa for instructive discussion from experimental viewpoints and Dr. Toga for useful discussion on the result of the Monte Carlo study. The present work was supported by the Elements Strategy

Initiative Center for Magnetic Materials (ESICMM) (Grant No. 12016013) funded by the Ministry of Education, Culture, Sports, Science and Technology (MEXT) of Japan, and was partially supported by Grants-in-Aid for Scientific Research C (Grants No. 18K03444 and No. 20K03809) from MEXT. The numerical calculations were performed on the Numerical Materials Simulator at the National Institute for Materials Science.

-
- [1] M. Sagawa and S. Hirosawa, *J. Mater. Res.* **3**, 45 (1988).
- [2] J. F. Herbst, J. J. Croat, F. E. Pinkerton, and W. B. Yelon, *Phys. Rev. B* **29**, 4176 (1984).
- [3] S. Hirosawa, Y. Matsuura, H. Yamamoto, S. Fujimura, M. Sagawa, and H. Yamauchi, *J. Appl. Phys.* **24**, L803 (1985).
- [4] A. V. Andreev, A. V. Deryagin, N. V. Kudrevatykh, N. V. Mushnikov, V. A. Reimer, and S. V. Terent'ev, *Zh. Eksp. Teor. Fiz.* **90**, 1042 (1986) [*Sov. Phys. JETP* **63**, 608 (1986)].
- [5] H. Kronmüller and K.-D. Durst, *J. Magn. Magn. Mater.* **74**, 291 (1988).
- [6] J. F. Herbst, *Rev. Mod. Phys.* **63**, 819 (1991), and references therein.
- [7] S. Sugimoto, *J. Phys. D: Appl. Phys.* **44**, 064001 (2011).
- [8] H. Kronmüller, *Phys. Status Solidi B* **144**, 385 (1987).
- [9] S. Hirosawa, M. Nishino, and S. Miyashita, *Adv. Nat. Sci.: Nanosci. Nanotechnol.* **8**, 013002 (2017).
- [10] H. Kronmüller and M. Fähnle, *Micromagnetism and the Microstructure of Ferromagnetic Solids* (Cambridge University Press, Cambridge, UK, 2003), and references therein.
- [11] J. Fischbacher, A. Kovacs, H. Oezelt, M. Gusenbauer, T. Schrefl, L. Exl, D. Givord, N. M. Dempsey, G. Zimanyi, M. Winklhofer, G. Hrkac, R. Chantrell, and N. Sakuma, *Appl. Phys. Lett.* **111**, 072404 (2017).
- [12] Y. Toga, M. Matsumoto, S. Miyashita, H. Akai, S. Doi, T. Miyake, and A. Sakuma, *Phys. Rev. B* **94**, 174433 (2016).
- [13] M. Nishino, Y. Toga, S. Miyashita, H. Akai, A. Sakuma, and S. Hirosawa, *Phys. Rev. B* **95**, 094429 (2017).
- [14] T. Hinokihara, M. Nishino, Y. Toga, and S. Miyashita, *Phys. Rev. B* **97**, 104427 (2018).
- [15] S. Miyashita, M. Nishino, Y. Toga, T. Hinokihara, T. Miyake, S. Hirosawa, and A. Sakuma, *Scr. Mater.* **154**, 259 (2018).
- [16] Y. Toga, M. Nishino, S. Miyashita, T. Miyake, and A. Sakuma, *Phys. Rev. B* **98**, 054418 (2018).
- [17] M. Nishino and S. Miyashita, *Phys. Rev. B* **100**, 020403(R) (2019).
- [18] I. E. Uysal, M. Nishino, and S. Miyashita, *Phys. Rev. B* **101**, 094421 (2020).
- [19] Y. Toga, S. Miyashita, A. Sakuma, and T. Miyake, *npj Comput. Mater.* **6**, 67 (2020).
- [20] M. Nishino, I. E. Uysal, and S. Miyashita (unpublished).
- [21] Q. Gong, M. Yi, R. F. L. Evans, B.-X. Xu, and O. Gutfleisch, *Phys. Rev. B* **99**, 214409 (2019).
- [22] Q. Gong, M. Yi, and B.-X. Xu, *Phys. Rev. Mater.* **3**, 084406 (2019).
- [23] Q. Gong, M. Yi, R. F. L. Evans, O. Gutfleisch, and B.-X. Xu, *Mater. Res. Lett.* **8**, 89 (2020).
- [24] S. C. Westmoreland, R. F. L. Evans, G. Hrkac, T. Schrefl, G. T. Zimanyi, M. Winklhofer, N. Sakuma, M. Yano, A. Kato, T. Shoji, A. Manabe, M. Ito, and R. W. Chantrell, *Scr. Mater.* **148**, 56 (2018).
- [25] S. C. Westmoreland, C. Skelland, T. Shoji, M. Yano, A. Kato, M. Ito, G. Hrkac, T. Schrefl, R. F. L. Evans, and R. W. Chantrell, *J. Appl. Phys.* **127**, 133901 (2020).
- [26] F. Wang and D. P. Landau, *Phys. Rev. Lett.* **86**, 2050 (2001).
- [27] D. Givord, A. Lienard, P. Tenaud, and T. Viadieu, *J. Magn. Magn. Mater.* **67**, L281 (1987).
- [28] J. L. García-Palacios and F. J. Lázaro, *Phys. Rev. B* **58**, 14937 (1998).
- [29] M. Nishino and S. Miyashita, *Phys. Rev. B* **91**, 134411 (2015).
- [30] E. Simanek and B. Heinrich, *Phys. Rev. B* **67**, 144418 (2003).
- [31] H. J. Skadsem, Y. Tserkovnyak, A. Brataas, and G. E. W. Bauer, *Phys. Rev. B* **75**, 094416 (2007).
- [32] V. Kamberský, *Phys. Rev. B* **76**, 134416 (2007).
- [33] K. Gilmore, Y. U. Idzerda, and M. D. Stiles, *Phys. Rev. Lett.* **99**, 027204 (2007).
- [34] K. Gilmore, Y. U. Idzerda, and M. D. Stiles, *J. Appl. Phys.* **103**, 07D303 (2008).
- [35] A. Brataas, Y. Tserkovnyak, and G. E. W. Bauer, *Phys. Rev. Lett.* **101**, 037207 (2008).
- [36] A. A. Starikov, P. J. Kelly, A. Brataas, Y. Tserkovnyak, and G. E. W. Bauer, *Phys. Rev. Lett.* **105**, 236601 (2010).
- [37] H. Ebert, S. Mankovsky, D. Kodderitzsch, and P. J. Kelly, *Phys. Rev. Lett.* **107**, 066603 (2011).
- [38] A. Sakuma, *J. Phys. Soc. Jpn.* **4**, 084701 (2012).
- [39] A. Sakuma, *J. Appl. Phys.* **117**, 013912 (2015).
- [40] P. A. Rikvold, H. Tomita, S. Miyashita, and S. W. Sides, *Phys. Rev. E* **49**, 5080 (1994).